Journal of the European Ceramic Society 20 (2000) 2575–2583

Fracture behaviour of alumina–calcium hexaluminate composites obtained by colloidal processing

A.J. Sánchez-Herencia, R. Moreno, C. Baudín *

Instituto de Cerámica y Vidrio, Ctra de Valencia Km 24,300, Arganda del Rey, 28500 Madrid, Spain

Received 14 September 1999; received in revised form 5 April 2000; accepted 11 April 2000

Abstract

Three different alumina (90 vol.%)–calcium hexaluminate (10 vol.%) composites have been prepared by colloidal processing of high purity starting powders in aqueous media and conventional sintering at 1500, 1550 and 1600°C. Calcium hexaluminate has been synthesised by high temperature reaction of alumina and calcium carbonate powders. The optimum dispersion conditions for the mixture have been selected from data for alumina and calcium hexaluminate slips studied independently. The microstructure of the obtained materials has been characterised by scanning electron microscopy. All of them showed a highly dispersed distribution of small CA_6 grains inside the alumina matrix. Grain size and shape of the alumina grains was highly dependent on the sintering temperature whereas the grain size of calcium hexaluminate remained almost constant. The fracture behaviour of the composites was analysed using Vickers indentation and optical and scanning microscopies. Higher loads could be applied to the composites without additional lateral cracking than to a monophase alumina material of the same average grain size. The fracture toughness values of the composites were highly dependent on the microstructure and for two of them values were larger than for the alumina material. Results have been discussed in terms of residual thermal stresses between the grains due to thermal expansion anisotropy.

Keywords: Al_2O_3–$CaAl_{12}O_{19}$; Composites; Mechanical properties; Microstructure-final

1. Introduction

The critical fracture energy and, therefore, toughness of alumina materials is highly dependent on grain size. This trend has been related to local stresses developed between grains due to thermal expansion anisotropy (TEA), as in other non-cubic and non-transforming ceramics.

Thermal expansion anisotropy stresses which develop upon cooling may assist in microcracking generation around the loaded crack tip. These microcracks constitute a mechanism of energy absorption and, for materials with grain size up to approximately half the value corresponding to spontaneous fracture, may increase the fracture toughness. Early theories proposed this toughening mechanism for alumina materials.[1–3]

Careful observations of the indentation crack paths in alumina materials representing a wide range of grain sizes showed that in fine-grained materials ($d < 5$ μm), the predominant fracture mode was intergranular and that the extent of transgranular fracture increased with increasing grain size. These variations of fracture morphology with grain size are opposite to those expected where microcracking is the dominant mechanism and suggest that crack branching plays an important role in the toughness increase with grain size.[4] Grain boundary microcracking due to TEA may act as initiation sites for crack branching.

Later in situ observations of cracks with well defined shapes during loading showed that crack interface bridging by interlocked grains behind the crack tip was responsible for crack stabilisation in all alumina materials with grain size larger than 5 μm.[5,6]

Crack bridging phenomena and, consequently, flaw tolerance in monophase ceramics may be enhanced only by scaling up the grain size. This way of toughness enhancement is limited by the amount of spontaneous microcracking that the material may stand without generalised failure.

Second phases with lower thermal expansion than that of the alumina matrix may enhance the effective-

* Corresponding author. Fax: +34-91-870-0550.

0955-2219/00/$ - see front matter
PII: S0955-2219(00)00123-0

ness and density of the bridges as observed in alumina–aluminium titanate composites.[7] Increasing the volume fraction and particle size of the second phase enhances flaw tolerance of the material, but this increase is also limited by spontaneous microcracking of the matrix due to the opening stresses that the second phase particles exert on the matrix walls.[8,9]

Calcium hexaluminate, $CaAl_{12}O_{19}$ (CA_6), is an interesting compound as a second phase in alumina based composites because it is thermodynamically compatible with alumina and it has the same average thermal expansion coefficient ($\approx 8.5\ 10^{-6}\ ^{\circ}C^{-1}$). But its thermal expansion behaviour is highly anisotropic ($\alpha_a = 7.3 \times 10^{-6}\ ^{\circ}C^{-1}$, $\alpha_c = 11.8 \times 10^{-6}\ ^{\circ}C^{-1}$).[10] Hence, thermal expansion mismatch between alumina and CA_6 particles may be expected.

Extensive work has been devoted to the study of CA_6 as a component of refractory materials but few papers deal with the fabrication or characterisation of alumina–CA_6 dense composites for structural applications.[10–13]

A series of fine grained ($\approx$5 μm) reaction sintered alumina–CA_6 composites containing different CA_6 amounts was studied[10,11] but toughness values did not show any benefit from the CA_6 particles in spite of their plate-like shape, a result attributed to the larger porosity present in the composite materials. The lower density was due to the fact that in situ formation of CA_6 during sintering involves a volume expansion during the formation of the different intermediate calcium–alumina compounds. Even though the critical temperature interval for fracture initiation during thermal shock tests of these composites was of the same order as that of monophasic alumina materials, the resistance to thermal shock damage of the composites was found to increase as the amount of CA_6 increased.[11]

The fracture behaviour of large grained ($\approx$20–30 μm) alumina–calcium hexaluminate composites prepared by reaction sintering[12,13] was studied using the indentation strength technique, revealing *R*-curve behaviour more pronounced as the shape factor of the CA_6 increased,[13] and this behaviour was attributed to crack bridging by the CA_6 grains. But an interesting feature of the fracture of these composites is that most CA_6 platelets were traversed by the crack. This happened despite the fact that debonding parallel to the alumina–CA_6 interfaces would be favoured due to thermal expansion mismatch and the plane parallel to the platelet faces (0001) is a cleavage one in the magnetoplumbite structure. Therefore, the number of intact CA_6 ligaments ready to bridge the wake of the crack was very small and toughening of these composites was limited.

In this paper, a different approach has been used to study the effect of CA_6 additions on the fracture behaviour of alumina. In principle, due to the thermal anisotropy of CA_6, some thermal mismatch between an alumina matrix ($\alpha_{avg} = 8.5 \times 10^{-6}\ ^{\circ}C^{-1}$) and CA_6 particles embedded in the matrix might be expected. Therefore, depending on orientation, stresses parallel or perpendicular to the interface between the CA_6 grains and the matrix would appear at least for some orientations. The objective of this work has been to establish the effect of these stresses on the fracture behaviour. To reach this objective, fine-grained alumina–CA_6 composites with a good dispersion of homogeneously sized and shaped CA_6 particles surrounded by the alumina matrix were needed.

In order to obtain such homogeneous composites, processing steps should be carefully controlled. Conventional forming by pressing cannot provide the control necessary to improve the microstructure. Alternatively, colloidal processing routes have demonstrated to be a powerful tool to obtain highly homogeneous mixtures of powders. However, very small effort has been devoted up to now for manufacturing alumina–CA_6 reliable ceramics by controlling the colloidal behaviour of well-dispersed slurries. In order to avoid segregation or agglomeration phenomena a rheological characterization of the starting powders and their mixtures is necessary. The degree of the dispersion will determine the homogeneity in the sintered body and the process reliability.

In this work a colloidal processing route for manufacturing homogeneous alumina–CA_6 composites is described. High purity commercial alumina and already reacted micrometer sized CA_6 powders have been dispersed in water and rheologically characterised. The compacts have been obtained by a colloidal filtration route and further conventional sintering. Special attention has been paid to the microstructural characterisation of the composite and to the effect of the microstructure on the fracture behaviour.

2. Experimental

2.1. Starting materials and slurries preparation

A commercial high purity (99.99%) alumina (Condea HPA 0.5, USA) and a calcium hexaluminate (CA_6) synthesised in the laboratory were used as starting powders for the composite materials.

Calcium hexaluminate was obtained by high temperature reaction of alumina and calcium carbonate (Merck, Germany, 99.0% purity). Stoichiometric concentrations were attrition milled for 4 h in isopropanol using alumina balls for a complete homogenisation. After mixing the powders were dried and sieved below 60 μm. The dried mixture was isostatically pressed at 200 MPa and calcined at 1600°C for 3 h and at 1650°C for 3 and 4 h. The reaction of CA_6 formation was followed by X-ray diffraction (XRD) using a Siemens D5000 diffractometer (Germany) to establish the best

conditions for complete reaction. The obtained XRD diagrams have been analysed using the ASTM diffraction files of corundum (46-1212), calcium hexaluminate (38-470), and the intermediate calcium aluminates ($CaAl_4O_7$: 23-1037, $Ca_2Al_{12}O_5$: 32-01). CA_6 compacts prepared using the selected optimum conditions were crushed and attrition milled with alumina balls in isopropanol and the evolution of the particle size distribution with the milling time was followed in order to obtain micron-sized particles. The powders to be used as starting materials for the composites were milled according to the results.

The density of the powders was measured by helium picnometry (Multipycnometer, Quantachrome, USA). Specific surface areas were determined by the one point N_2 adsorption method (Monosorb, Quantachrome, USA). Particle size distributions were determined with a light scattering system (Mastersizer S, Malvern, UK) using a liquid dispersion unit with distilled water.

Al_2O_3 slips and CA_6 slips were prepared to a solid loading of 70 wt.% (38 and 39 vol.%, respectively) in deionised water with different concentrations of a carbonic acid based polyelectrolyte as deflocculant (Dolapix CE64, Zschimmer-Schwarz, Germany), and the dispersion conditions for the slips were determined. For the Al_2O_3–10 vol.% CA_6 composites, 70 wt.% slips were prepared using the optimum dispersing conditions for each component in the mixture following a two step procedure. Firstly, the CA_6 was energetically stirred in the total volume of water in the presence of the total amount of dispersant required for homogenising the mixture using a high shear mixer (Silverson, L2R, UK). Secondly, after complete coverage of the dispersant onto the CA_6 particles, the Al_2O_3 powder was then added. This mixture was homogenised by ball milling overnight using alumina jar and balls.

For rheological measurements a rheometer (Haake, RS50, Germany) with a double cone/plate geometry was used. Measurements were performed by changing shear rate from 0 to 1000 s^{-1} for 2 min, for both the up and down ramps with 1 min at the maximum rate. Temperature was maintained constant at 25°C.

2.2. Samples preparation and characterisation

The well-dispersed Al_2O_3–10 vol.% CA_6 slips were cast on plaster of Paris moulds to obtain the green bodies. Samples were left to dry in air for at least 48 h and then sintered in the range of temperatures 1500–1600°C for 2 h (heating and cooling rates 5°C/min).

Archimedes' method, using mercury and water, respectively, was used to determine green and sintered densities.

Sintered samples were polished using diamond paste down to 1 μm for microscopic and indentation experiments. Scanning electron microscopy (DSM 950, Zeiss, Germany) was performed on thermally etched (1450°C–1 h, heating and cooling rates 10°C/min) surfaces. To differentiate alumina from calcium hexaluminate, EDX was performed to obtain Ca X-ray maps and single particles or groups of particles of sufficient size (>2 μm) were also analysed. With the same purpose backscattered images were used. The average particle size of alumina was determined quantitatively using the linear intercept method on SEM micrographs and the aspect ratio of these particles was calculated as the ratio of the length to the width directly measured on the micrographs. The approximate size of the CA_6 particles was directly measured on the micrographs. These measurements were performed on two different random areas of 86×97 μm for each sample, which included at least 200 grains.

Dynamic Young's modulus was calculated from the resonance frequency of bars tested in flexure using the impact method (Grindosonic, Belgium).

Indentations were performed on polished samples using a Vicker's indenter and maintaining the fixed load for 15 s (LECO, USA). Loads between 10 and 500 N were applied and the indentation cracks were observed using optical (Zeiss, Germany) and scanning microscopes. Crack lengths corresponding to well defined indentations (no chipping, only two perpendicular lateral cracks) were measured by optical microscopy and values were used to calculate toughness using the equation of Ref. 14.

3. Results and discussion

3.1. Calcium hexaluminate synthesis

The X-ray diffraction spectra of powders milled from the alumina–calcium carbonate compacts thermally treated at 1600 and 1650°C were analysed, The compacts treated at 1600°C showed some residual alumina, as an indication that the reaction was not complete. The peaks corresponding to the alumina disappeared in the XRD diagram of the sample treated at 1650°C and only CA_6 was detected. The diagrams of the samples treated at 1650°C for 3 and 4 h were identical. Therefore, the temperature of the heat treatment used to synthesise the CA_6 was 1650°C.

The evolution of the particle size distribution of ground CA_6 powders versus attrition milling time was followed. After 6 h (Fig. 1a), the particle size distribution was bimodal, centered at 0.3 and 1.1 μm, and no further decrease of the particle size with longer milling times (8 h) was obtained. The size bimodality of the powders, plotted in Fig. 1a, can be observed in the SEM micrograph of the powder shown in Fig. 1b. The alumina powders presented a unique particle size distribution with average particle size of 0.3 μm (Fig. 1a). Apart

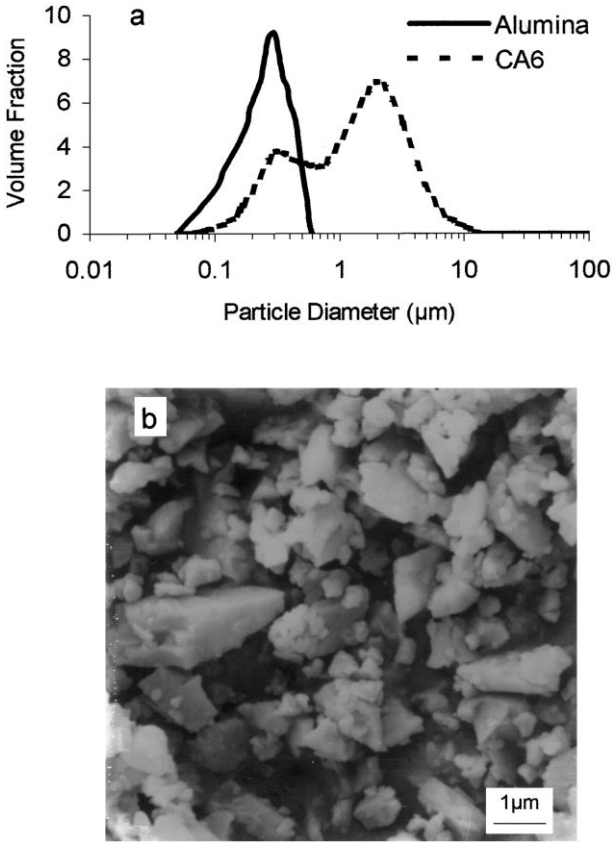

Fig. 1. (a) Particle size distributions of alumina and grounded CA_6 powders after milling; (b) micrograph of the CA_6 after milling where bimodality is clearly observed.

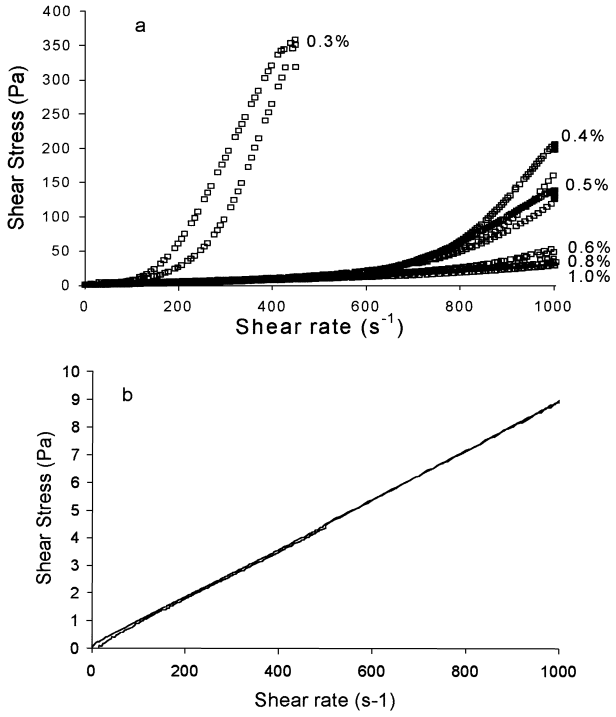

Fig. 2. Flow curves of the studied slips: (a) CA_6 as a function of the dispersant concentration; (b) alumina + 10 vol.% CA_6 with 0.6 wt.% of dispersant.

from size distribution, the alumina and CA_6 powders differ in density values (3.69 and 3.88 g/cm^3 for CA_6 and alumina, respectively) and specific surface area (3.1 and 9.5 m^2/g for CA_6 and alumina, respectively).

3.2. Rheological behaviour and fabrication of the green compacts

For the preparation of the mixtures the rheological behaviour of slips of each material was previously characterised. Aqueous slips with a solid loading of 70 wt.% were prepared by adding concentrations of deflocculant between 0.2 and 1.0 wt.% referred to solids. Fig. 2a shows the flow curves corresponding to the CA_6 slips. They behave as dilatant at high shear rates. In addition, for deflocculant contents up to 0.6 wt.%, there is a noticeable time dependency. The dilatancy significantly decreases for dispersant additions of 0.7 wt.%. The viscosity is reduced for 0.8 wt.%, and no significant reduction is achieved for larger deflocculant contents.

For alumina, well-dispersed slips were obtained for deflocculant contents of 0.6 wt.% and very small differences were found depending on the concentration. The slips presented a nearly Newtonian behaviour with very low viscosities (< 10 mPa s). In principle, the rheological behaviour of a mixture depends mainly on that of the major constituent, in this case alumina. Moreover, the optimum amount of dispersant for the alumina slip is in the same range as that for the CA_6 one. But, the differences in the powder characteristics mentioned above (shape, specific surface area) might be responsible for preferential adsorption of the dispersant on the major constituent. In order to assure a complete coverage of dispersant (0.6 wt.%) to the surface of CA_6 particles, the slips were prepared using a two step method, Firstly, the CA_6 powder was added to the water containing the total deflocculant amount. In a second step, the major phase was added and homogenised in the ball mill. Fig. 2b shows the flow curve of the alumina + 10 vol.% CA_6 with the 0.6% of dispersant. It is clearly observed that a Newtonian behaviour is obtained with a viscosity value as low as 10 mPa s.

3.3. Microstructure

The green density of the slip-cast samples was 2.61 g/cm^3, which represents 66% of the theoretical density of the mixture (3.69 g/cm^3). This high density is possible because of the bimodal particle size distribution and the good dispersion of the mixture.

The homogeneity of the sintered composite material can be observed in Fig. 3. In this micrograph, taken

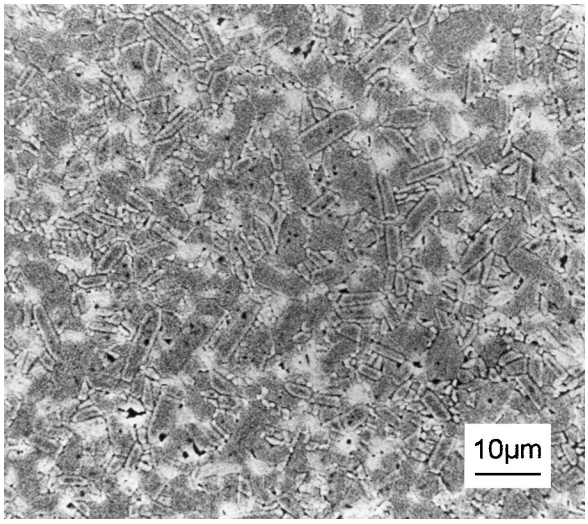

Fig. 3. Backscattered SEM micrographs of the alumina–CA_6 composite sintered at 1500°C. The bright areas correspond to CA_6 grains.

from the backscattered electron image, the CA_6 grains can be distinguished because they are brighter than the alumina ones; the Ca X-ray map confirmed this observation. CA_6 grains are very small and are homogeneously dispersed inside the alumina matrix.

The sintering temperature did not affect density values of the obtained materials and all values were in the range 99–99.5‰.

Fig. 4 shows micrographs of the samples sintered at the three different temperatures. The quantitative microstructural analysis of these samples is summarised in Table 1.

The three materials present the same kind of microstructure (Fig. 4, Table 1), constituted of equidimensional and small (<2 μm) CA_6 grains embedded in a bimodal alumina matrix in which the smaller grains ($\leqslant 3$ μm) are equidimensional and the larger ones are tabular. The sintering temperature has a major role in the development of the microstructure, mainly regarding to the size and shape of the alumina grains, as deduced from quantitative values in Table 1. For the materials treated at the lower temperatures (1500 and 1550°C, Fig. 4a and b, respectively) there are not large differences in average alumina grain size ($D_{50} = 3.3$–3.4 μm) and the size of the smallest grains ($D = 0.8$–2 μm). But a clear increase of both parameters ($D_{50} = 5$ μm, $D = 1$–3 μm) is observed for the material treated at 1600°C (Fig. 4c). The tabular growth of the alumina grains is favoured at 1500 and 1550°C (shape factors = 2–3) whereas in the compacts treated at 1600°C the aspect ratio is lower (shape factor = 1.2) and pore trapping occurs, revealing exaggerated grain growth (Fig. 4c). In order to evaluate the influence of CA_6 as a second phase in the Al_2O_3 based material, a monolithic Al_2O_3 material was prepared controlling the sintering conditions to obtain a similar grain size. This was achieved for the same Al_2O_3 powder after sintering at 1600°C/1 h.[15] The grains of the monolithic alumina material are mostly equidimensional (Fig. 4d) and the average size determined for this material was 5 μm. Some of the largest grains in this material are tabular, with lengths >5 μm.

The development of faceted grains in ceramics is often associated with the presence of a wetting boundary phase, which leads to slow growth rates which are responsible for anisotropic growth, but no liquid phase formation is expected at the sintering temperatures in the high purity compacts studied here, as liquid phase in biphasic alumina–CA_6 composites does not form up to temperatures over 1800°C.[16] Moreover, when transient liquids are formed in reaction sintered alumina–CA_6 materials, tabular growth of CA_6 and not of alumina is favoured.[10,11] Alternatively, thermodynamics may play a role in stimulating the development of elongated grains if the grain boundary energy depends upon grain boundary plane orientation, as it occurs in pure alumina materials.[17] In the composites studied here, the CA_6 particles may cause pinning leading to preferential grain growth at the lower sintering temperatures (1500–1550°C), and this effect would be overcome when the sintering temperature increases and leads to larger grain growth rates as in the case of the material sintered at 1600°C.

3.4. Mechanical behaviour

Dynamic Young's modulus values for the three composites were in the range 363±9 GPa, which agrees well with the Voight limit for the Young's modulus of composite materials considering the values of 380 GPa for alumina and 260 GPa for dense monophase calcium hexaluminate (260±10 GPa[18]). Therefore, no extensive spontaneous cracking takes place in these materials during cooling from the sintering temperature.

Table 1
Quantitative microstructural features of the studied composite materials

Sintering temperature	Average grain size (μm)	CA_6 range of sizes (μm)	Length of the tabular alumina grains	Shape factor of the tabular alumina grains
1500	3.3±0.3	0.8–2	3–8	2 0±0.2
1550	3.4±0.3	1–2	3–10	3±0.3
1600	5±0.3	1–2.5	5–10	1.2±0.1

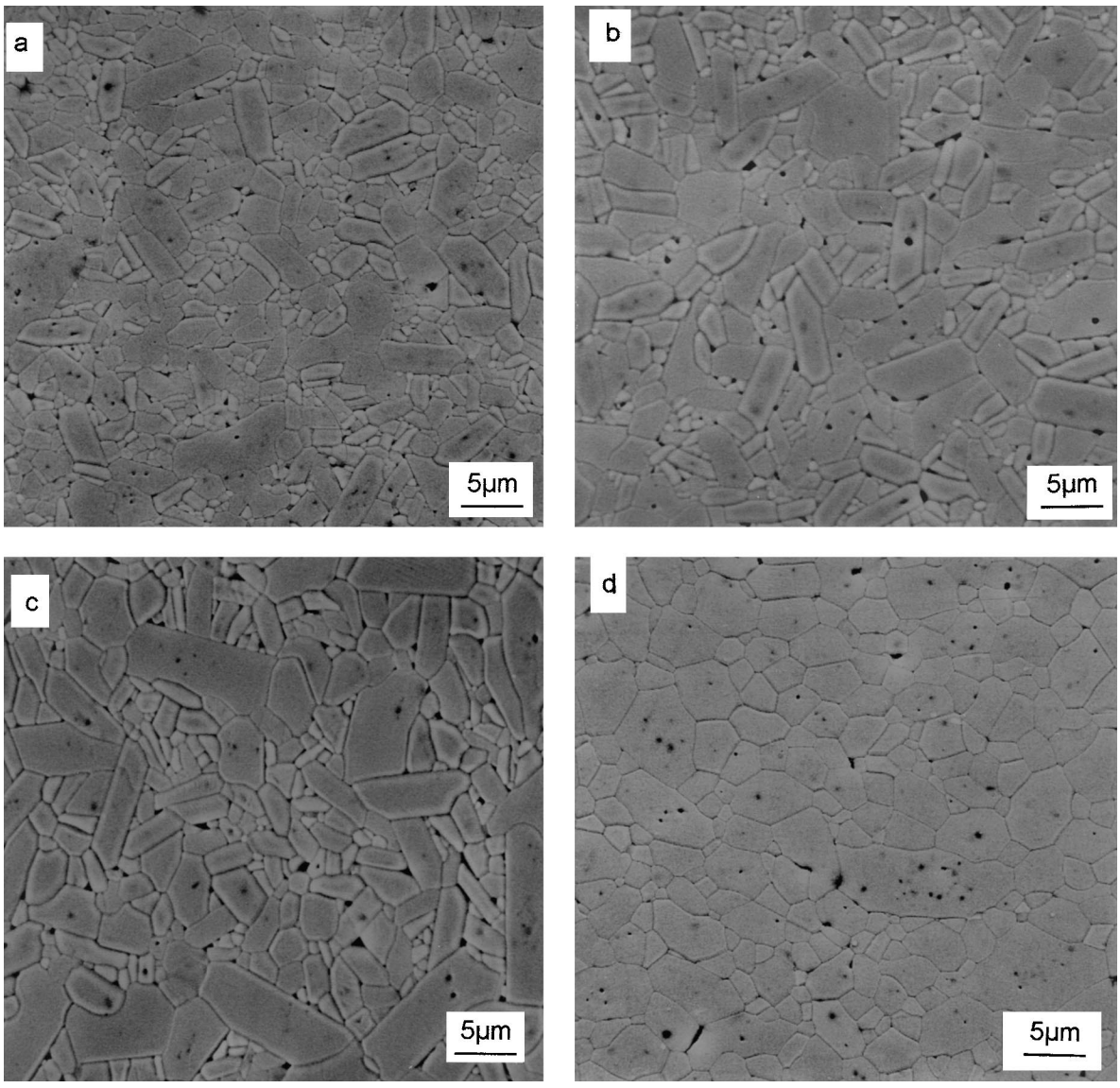

Fig. 4. SEM micrographs of polished and thermal etched surfaces of the alumina–CA_6 composites sintered at different temperatures and of the monophase alumina material: (a) 1500°C; (b) 1550°C; (C) 1600°C; (d) alumina sintered at 1650°C/1 h.

The four studied materials had different behaviour under Vickers' indentation. The maximum load that could be applied to the pure alumina material without extensive chipping was 200 N and no variation of toughness as a function of load (50, 100 and 200 N) was found. Conversely, loads up to 500 N could be applied to the alumina–CA_6 compacts sintered at 1500 and 1550°C, and up to 300 N to the one sintered at 1600°C without chipping (Fig. 5a and b), indicating that no additional cracking occurred under the indentation.

An increase of toughness values with the applied load was found for the three composites in all cases with well developed cracks ($C > 2.5$ a, $c = 0.5$ radial crack size, $a = 0.5$ diagonal of the plastic zone); this feature was not observed in the alumina material. The fact that this dependence does not take place in the alumina material, which microstructure is similar to that of the composite sintered at 1600°C (Fig. 4c and d) implies that it should be related to the presence of CA_6. For the two composites sintered at the highest temperatures the toughness values in the constant region (loads larger than 200 and 300 N, 1550 and 1600°C, respectively) are larger than the obtained constant value for the alumina material (Fig. 6). The larger toughness values of the composite sintered at the highest temperature when compared to those corresponding to the alumina material with similar microstructure reveal that an energy absorbing mechanism is taking place in the composites during fracture.

Characteristic crack patterns for the indented samples are shown in Fig. 7. The crack paths in the pure alumina material were straight and showed a mixture of intergranular and transgranular modes (Fig. 7a), being very similar to that reported by other authors for fine-grained materials.[4] In the composite materials (Fig. 7b–d),

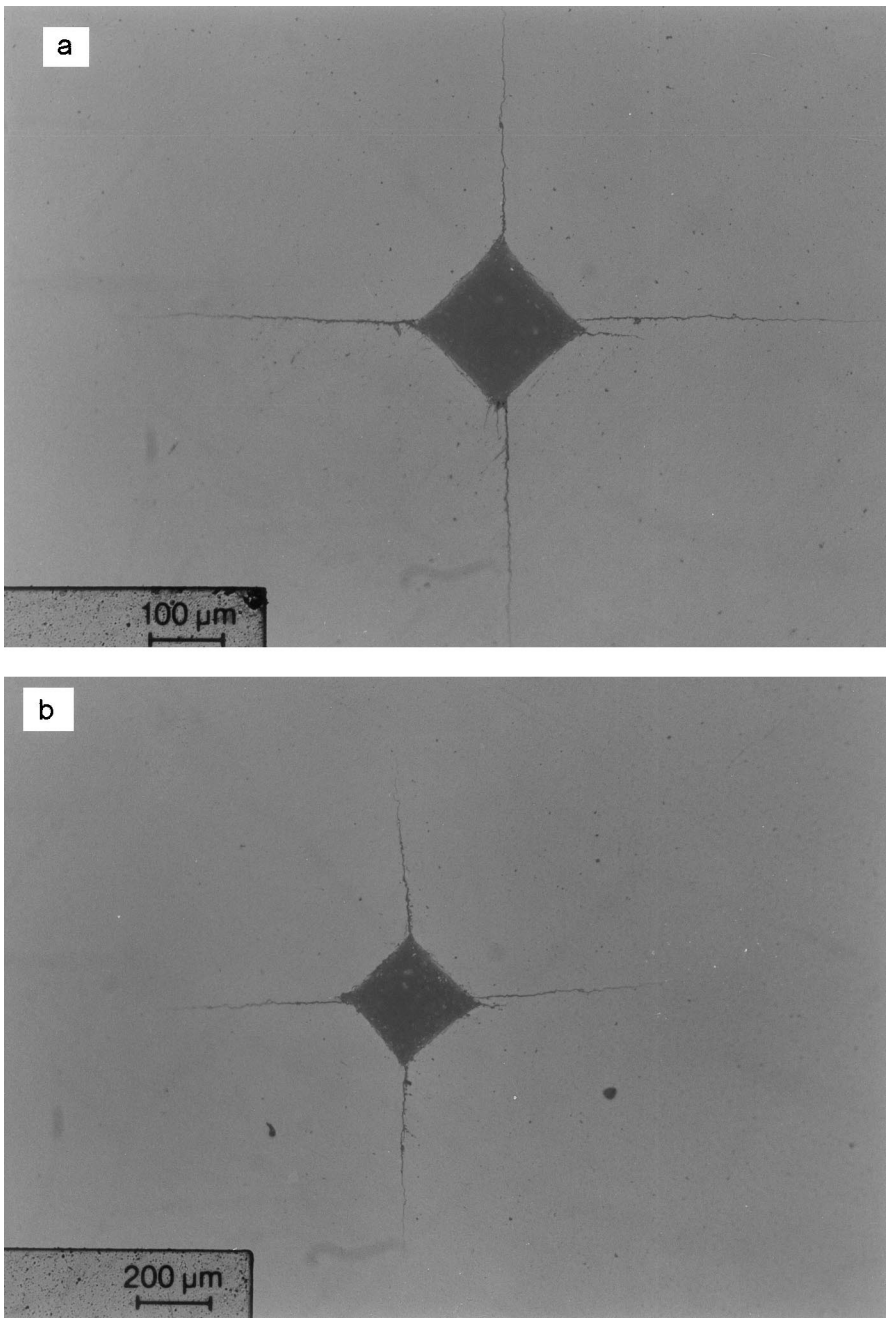

Fig. 5. Optical micrographs of indentations over the polished surfaces of the alumina–CA_6 composites sintered at different temperatures showing the indentation cracks and the absence of chipping: (a) 1550°C, indentation load 500 N; (b) 1600°C, indentation load 300 N.

the fracture mode of the alumina matrix was also mixed inter-transgranular but, the crack changed its direction of propagation, even traversing the alumina grains, to link areas where intergranular fracture around the small grains (mostly CA_6) occurred, as seen in detail in Fig. 7d. This feature is similar to that observed in alumina based composites in which crack bridging takes place. In these materials, crack propagation occurs in two steps: (a) opening of a microcrack ahead of the crack tip, (b) joining of the microcrack to the primary crack.[19] The same fracture processes might be the energy absorbing mechanisms in the composites as the observed dependence of toughness on microstructure is in agreement with the crack bridging hypothesis: the coarse grained composite material sintered at 1600°C presents the largest toughness values (Figs. 4 and 6, Table 1) and for the two composites sintered at the lower temperatures, which present similar average grain size, an increase of toughness with shape factor occurs (Figs. 4 and 6, Table 1).

Due to differences between the average expansion coefficient of the alumina matrix and the *c*-axis expansion

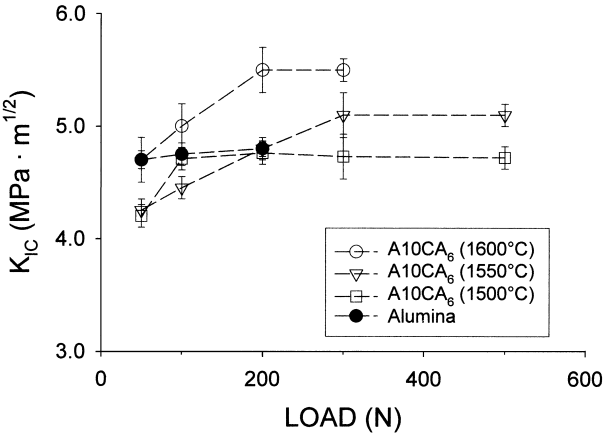

Fig. 6. Toughness values as a function of the applied load for the studied materials.

coefficient of CA_6, thermal mismatch stresses perpendicular to the Al_2O_3/CA_6 interfaces are expected. Such stress system does not add to the indentation load to develop additional lateral cracking across the matrix, and, in fact, the composite materials support larger loads than the monophase alumina material without chipping (Fig. 5). This stress system leads to microcracking around the CA_6 particles when loading, and these microcracks constitute the initiation sites for crack branching. The alumina grains located between two areas of intergranular fracture would act as elastic bridges before being traversed by the primary crack and crack bridging will be responsible for the observed change in crack direction in the surface of the indented samples (Fig. 7b–d).

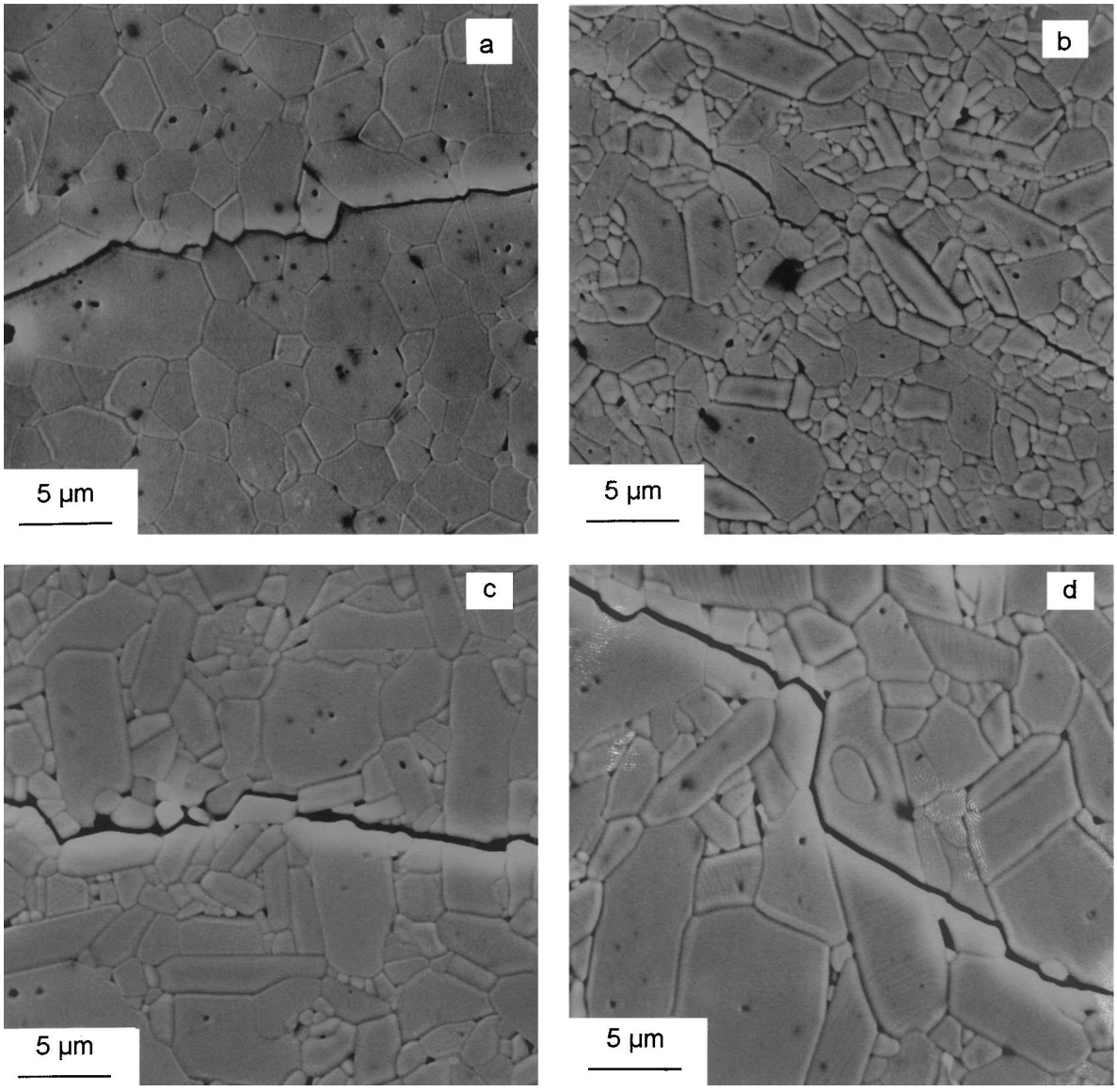

Fig. 7. Indentation crack path in the studied materials, SEM micrographs of thermally etched polished and indented surfaces: (a) alumina; (b) alumina–CA_6 composite sintered at 1500°C; (c) alumina–CA_6 composite sintered at 1550°C; (d) alumina–CA_6 composite sintered at 1600°C.

4. Conclusions

Alumina-based composites with a homogeneous dispersion of small (≈μm) and equidimensional calcium hexaluminate particles can be obtained by colloidal processing and conventional sintering. The dispersion of CA_6 inside the alumina matrix can be controlled using rheological parameters when the complete adsorption of the dispersant on the minor phase (CA_6) is assured. In the range of sintering temperatures 1500–1600°C, CA_6 grains are equidimensional and small sized and the size and shape of the grains of the Al_2O_3 matrix is controlled by the sintering process.

The presence of CA_6 as a second phase affects the fracture behaviour of the alumina matrix. First, larger indentation loads can be applied to the composites, compared to a monophasic alumina material with similar grain size, without multiple cracking and, second, larger toughness values are obtained for the composites than for the alumina material.

The dependence of the toughness values of the composites on their microstructural differences (grain size and shape) as well as the crack path features agree with a hypothesis of crack bridging phenomena occurring in the composites originated from microcracking around the CA_6 particles.

Acknowledgement

This work has been supported by CICYT (Spain) under contract MAT96-0408.

References

1. Rice, R. W., Freeman, S. W. and Becher, P. F., Grain size dependence of fracture energy in ceramics; I, experiment. *J. Am. Ceram. Soc.*, 1981, **64**, 345–349.
2. Rice, R. W. and Freiman, S. W., Grain size dependence of fracture energy in ceramics; II, a model for non-cubic materials. *J. Am. Ceram. Soc.*, 1981, **64**, 350–354.
3. Claussen, N., Mussler, B. and Swain, M. V., Grain-size dependence of fracture energy in ceramics. *J. Am. Ceram. Soc.*, 1982, **65**, C14–C16.
4. Mussler, B., Swain, M. V. and Claussen, N., Dependence of fracture toughness of alumina on grain size and test technique. *J. Am. Ceram. Soc.*, 1982, **65**, 566–572.
5. Swanson, P. L., Fairbanks, C. J., Lawn, B. R., Mai, Y.-W. and Hockey, B.J., Crack-interface grain bridging as a fracture resistance mechanism in ceramics: I, experimental study on alumina. *J. Am. Ceram. Soc.*, 1987, **70**, 279–289.
6. Chantikul, P., Bennison, S. J. and Lawn, B. R., Role of grain size on the strength and R-curve properties of alumina. *J. Am. Ceram. Soc.*, 1990, **73**, 2419–2427.
7. Padture, N. P., Bennison, S. J. and Chan, H. M., Flaw tolerance and crack-resistance properties of alumina–aluminum titanate composites with tailored microstructures. *J. Am. Ceram. Soc.*, 1993, **76**, 2312–2320.
8. Lawn, B. R., Padture, N. P., Braun, L. M. and Bennison, S. J., Model for toughness curves in two-phase ceramics: I, basic fracture mechanics. *J. Am. Ceram. Soc.*, 1993, **76**, 2335–2340.
9. Padture, N. P., Runyan, J. L., Bennison, S. J., Braun, L. M. and Lawn, B. R., Model for toughness curves in two-phase ceramics: II, microstructural variables. *J. Am. Ceram. Soc.*, 1993, **76**, 2241–2247.
10. Criado, E. Caballero, A. and Pena, P., Microstructural and mechanical properties of alumina–calcium hexaluminate composites. In *High Tech Ceramics*, ed. Vicenzini. Elsevier Science Publishers B.V., Amsterdam, The Netherlands, 1987, pp. 2279–2289.
11. Criado, E. and Baudmn, C., Comportement au choc thermique des matériaux réfractaires d'alumine–hexaluminate calcique. Presented at *Refractaires et Sollicitations Thermomecaniques*. Soc. Francaise de Céramique, Paris, France, 1990.
12. An, L., Chan, H. M. and Soni, K. K., Control of calcium hexaluminate grain morphology in in-situ toughened ceramic composites. *J. Mater. Sci.*, 1996, **31**, 3223–3229.
13. An, L. and Chan, H. M., R-curve behavior of in-situ toughened Al_2O_3:$CaAl_{12}O_{19}$ ceramic composites. *J. Am. Ceram. Soc.*, 1996, **79**, 3142–3148.
14. Miranzo, P. and Moya, J. S., Elastic/plastic indentation in ceramics: a fracture toughness determination method. *Ceram. Int.*, 1984, **10**, 147–152.
15. Moreno, R., Miranzo, P., Moya, J. S. and Requena, R., Microstructural and sintering behaviour of different alumina powders. In *Euroceramics — II, Vol. 1, Basic Science and Processing of Ceramics*, ed. G. Ziegler and H. Hausner. DKG, Köln, 1991, pp. 471–475.
16. Hallstedt, B., Assessment of the CaO–Al_2O_3 system. *J. Am. Ceram. Soc.*, 1990, **73**, 15–23.
17. Rodel, J. and Glaeser, A. M., Anisotropy of grain growth in alumina. *J. Am, Ceram. Soc.*, 1990, **73**, 3292–3301.
18. Criado, E., Pena, P. and Caballero, A., Influence of processing method on microstructural and mechanical properties of calcium hexaluminate compacts. In *Science of Ceramics* 14, ed. Taylor. The Institute of Ceramics, Shelton, UK, 1988, pp. 193–198.
19. Rodel, J., Crack closure forces in ceramics: characterization and formation. *J. Eur. Ceram. Soc.*, 1992, **9**, 323–334.